International Journal of Greenhouse Gas Control 76 (2018) 208–214

Contents lists available at ScienceDirect

International Journal of Greenhouse Gas Control

journal homepage: www.elsevier.com/locate/ijggc

NO_X formation in oxy-fuel combustion of lignite in a bubbling fluidized bed – Modelling and experimental verification

Matěj Vodička[a,*], Nils Erland Haugen[b], Andrea Gruber[b], Jan Hrdlička[a]

[a] Czech Technical University in Prague, Faculty of Mechanical Engineering, Department of Energy Engineering, Technická 4, 166 07 Prague, Czech Republic
[b] SINTEF Energy Research, Kolbjørn Hejes vei 1a, NO-7465, Trondheim, Norway

ARTICLE INFO

Keywords:
Oxy-fuel combustion
Bubbling fluidized bed
NO_x
Emissions
Modelling

ABSTRACT

This paper reports results of experimental and numerical studies of NOx formation in a 30 kW_{th} lab-scale bubbling fluidized bed running in oxy-fuel mode. The numerical model is based on the GRI-mech 3.0 mechanism to compute the kinetics of homogeneous reactions of volatiles and char combustion products and takes into account the flue gas recirculation. The impact of the oxygen excess and of the fluidized bed temperature was examined. Both the numerical simulations and the experiments shown a significant correlation of NO_X formation with the excess of oxygen, where a higher oxygen concentration enhances the fuel-bound nitrogen oxidation to NO_X. It was also found that there is no correlation of the NOx formation and resulting emissions with the fluidized bed temperature in temperature range typical for bubbling fluidized bed combustors (840–960 °C), but the numerical simulations showed an increased NO_X concentration when the temperature raised more (up to 1360 °C). The agreement of experimental and numerical results shows that the numerical model can provide useful insight into the mechanism of NO_X formation.

1. Introduction

The majority of the world countries is obliged to reduce emissions of greenhouse gases thanks to countersigning the United Nations Framework Convention on Climate Change (United Nations and Canada, 1992). Carbon dioxide (CO_2), which belongs to this group of gases, is emitted from a large number of different applications, where one of the main sources is the fossil fuel based power producing industry. Several technologies (commonly called 'carbon capture and storage' or 'carbon capture and sequestration' (CCS) and 'carbon capture and utilization' (CCU)) were developed to reduce the CO_2 emissions from power production. One of the most promising carbon capture technologies is oxy-fuel combustion. Here, almost pure oxygen is used to oxidize the fuel, which means that almost no nitrogen is present in the combustion zone. As a result, the flue gas consists primarily of CO_2 and water vapour, which can be easily separated by condensation. This means that the CO_2 capture process itself is much straighter forward than for so-called post-combustion capture, where nitrogen is still present in the hot flue gas. This easy capture comes, however, at the penalty of an expensive and non-flexible oxygen production. A comprehensive review of the oxy-fuel combustion was published by Toftegaard et al. (2010)

Besides CO_2 and water vapour, the flue gas contains other trace components that need to be removed prior to CO_2 compression. One of them are nitrogen oxides (NO_X), particularly nitric oxide (NO) and nitrogen dioxide (NO_2), a group of pollutants that are also produced in combustion processes. The nitrous oxide (N_2O) does not belong to the NO_X group by definition in legislation, but it is a greenhouse gas and its emissions can be significant in fluidized bed combustion (Glarborg et al., 2003). The mechanisms of NO_X formation, as well as its reduction measures, are well known for air-fired combustion, even for bubbling fluidized bed combustors (BFBCs) (Johnsson, 1994; Skopec et al., 2015; Mahmoudi et al., 2010; Jensen et al., 1996; Konttinen et al., 2013). The situation is, however, different in oxy-fuel mode. The species present in the combustion zone occur in different concentrations than they do in air firing mode, which significantly affects the NO_X formation. Because of the absence of the molecular nitrogen N_2, which is normally brought to the combustor with the combustion air, the nitrogen oxides are produced primarily from the fuel-bound nitrogen and therefore only negligible formation through the thermal and prompt mechanism takes place.

1.1. Fuel-nitrogen chemistry in air-combustion

In the furnace, the fuel is thermally decomposed producing volatile and char compounds. The fuel-bound nitrogen is distributed between

* Corresponding author.
E-mail address: matej.vodicka@fs.cvut.cz (M. Vodička).

https://doi.org/10.1016/j.ijggc.2018.07.007
Received 1 September 2017; Received in revised form 25 June 2018; Accepted 5 July 2018

Nomenclature

Abbreviations

BFBC	Bubbling fluidized bed combustor
FGR	Flue gas recirculation
PFR	Plug flow model

Symbols

LHV	[MJ/kg] Low heating value
O_2/CO_{2_IN}	[-] Ratio of the O_2 and CO_2 volumetric fraction in the inlet gas
$res._{FB}$	[s] Residence time of the gas in the fluidized bed
$res.t_{freeb}$	[s] Residence time of the gas in the freeboard
$res.t_{overall}$	[s] Residence time of the gas in reactor
t_{FB}	[°C] Fluidized bed temperature
t_{OUT}	[°C] Temperature at the exit of the reactor
t_{FGR}	[°C] Temperature of the recirculated flue gas
u_0/u_{mf}	[-] Ratio of the superficial gas velocity and the minimum fluidizing velocity
z	[m] Height of the reactor
ω_{CO}	[ppmv] Volumetric fraction of CO in dry flue gas
ω_{CO2}	[vol. %] Volumetric fraction of CO_2 in dry flue gas
ω_{NOx}	[ppmv] Volumetric fraction of NOX in dry flue gas
ω_{O2}	[vol.%] Volumetric fraction of O_2 in dry flue gas

chars and volatiles depending on the fuel structure and devolatilisation conditions, such as temperature, heating rate, concentration of oxygen or residence time. The most important volatile nitrogen compounds are HCN, NH_3 and tars (volatile organic species condensing at room temperature) with amine or nitro groups and heterocyclic structures (Glarborg et al., 2003). These are simultaneously oxidized and it is considered that the HCN and NH_3 are the main sources of NO_X and N_2O. The tar-nitrogen is homogeneously oxidized to HCN, NH_3, NO, N_2O and N_2, but nitrogen can be present also in soot (Johnsson, 1994). It is difficult to determine the exact composition of volatiles, since the products of devolatilisation are subsequently consumed in the combustion process and do not remain as stable products. To describe initial stages of devolatilisation and tar reactions, pyrolysis under proper conditions, or single particle combustion, may give valuable inputs (Johnsson, 1994).

Li et al. (1996) studied the pyrolysis of lignite and bituminous coal in a bubbling fluidized bed reactor and observed that in case of lignite, most of the NH_3 and HCN is released during the primary pyrolysis of fuel with the HCN to NH_3 ratio being near unity. The secondary pyrolysis of char and tar-products did not change their yields significantly. Both the HCN and NH_3 formation were temperature dependent with maximum NH_3 yield at approx. 800 °C and increasing HCN formation tendency up to 1000 °C. However, authors observed a decomposition of NH_3 by reactor materials (zircon sand and stainless steel) at temperatures above 700 °C (Li and Nelson, 1996) and concluded, that the yields of NH_3 could be higher than they measured. Winter et al. (1996) studied the devolatilisation of coal in a single particle combustion reactor while analysing the flue gas composition using FTIR spectrometer and they did not detect NH_3 in a significant amount at all.

The oxidation of char-N is a complex and difficult to describe process consisting of various heterogeneous and subsequent homogenous reactions. The products of char-N oxidation comprise of a number of species (NO, N_2O, HCN, NH_3, HCNO, N_2) (Glarborg et al., 2003).The conversion of char-N to NO vary from 30% to almost 100% and it is presumed that NO is the major product of char-N oxidation (Glarborg et al., 2003). The active surface of char may also catalyse a number of reactions either NO forming or reducing, e.g. the reduction by CO or H_2 and the oxidation of NH_3 to NO.

1.2. NO_X in the oxy-fuel-combustion process

The changes in combustion atmosphere when changing from air fired to oxy-fuel fired combustion significantly influences the nitrogen chemistry. The near absence of molecular nitrogen N_2 is obviously of importance for the thermal and prompt NO_X formation, however, the dominance of CO_2 and H_2O and high relative concentration of combustion products affects the oxidation of fuel-bound nitrogen as well. Zhu et al. (2015) examined the effect of the water vapour introduction into the fluidized bed on the NO_X formation. They concluded that the H_2O addition to combustion agent enhances the NO_X reduction at low to moderate (up to 30 vol. %) oxygen concentrations at the inlet gas due to inhibited release of volatile N-species. At higher oxygen concentrations, the H_2O oxidation would tend to form more OH radicals which would result in increased NO_X formation compared to the situation without H_2O addition. Duan et al. (2011) studied the impact of a CO_2 atmosphere on NO_X precursor formation using tube furnace and FTIR gas analyser. They observed, that CO_2 influences both the NH_3 and HCN formation. The HCN yields were significantly enhanced in comparison to in an Ar atmosphere, whereas the NH_3 yields were suppressed. Giménez-López et al. (2010) studied HCN oxidation in an O_2/CO_2 atmosphere, corresponding to oxy-fuel combustion, and observed a considerable inhibition in comparison to the air-combustion. This inhibition of HCN formation is due to the competitive reaction of CO_2 and hydrogen radicals. As a result, depressed fuel-N/NO_X conversion ratio in the oxy-fuel regime can be expected, which was confirmed by Lupiáñez et al. (Lupiáñez et al., 2013) in a 90 kW_{th} BFBC.

According to Normann et al. (Normann et al., 2009), the elevated CO_2 concentration can also lead to changes in the radical pool of the combustion process, mainly through reaction

$$CO_2 + H \longleftrightarrow CO + OH. \quad (1)$$

Here, the higher concentration of hydroxyl radicals (OH) can promote the formation of NO from volatile-N, but also, as mentioned above, the CO can reduce the NO in the proximity of particles through reaction (Lupiáñez et al., 2013)

$$NO + CO \leftrightarrow \frac{1}{2}N_2 + CO_2 \quad (2)$$

This reaction can be particularly significant, since the formation of CO in oxy-fuel combustion is enhanced by the heterogeneous Boudouard reaction that uses the unburned fuel char

$$CO_2 + C^{(S)} \longleftrightarrow 2CO \quad (3)$$

which can also lead to another reduction of NO_x emission (Normann et al., 2009).

Zhou et al. (2018) studied the conversion of fuel-N to NO during devolatilization and char combustion in a oxy-fuel combustion atmosphere using a lab-scale flow tube reactor and observed that formation of NO is promoted by a temperature increase in the range 700–900 °C, both from the volatile- and char-N oxidation. However, while the impact on the volatile-N to NO conversion ratio was very small, the formation of NO from char-N seemed to be very temperature-sensitive. The temperature of the burning char particle is primarily dependent on the concentration of O_2 and on the char particle size (Svoboda et al., 2004). Within an oxy-fuel combustion atmosphere, the diffusivity of O_2 towards the char particle is lowered, which can, together with the enhanced gasification, decrease the temperature of the burning char particle compared to the air-combustion atmosphere (Bhunia et al., 2017; Salinero et al., 2018). This decrease is most dominant at higher

temperatures but it is significant even for the typical bubbling fluidized bed temperature range. The NO_X formation from combustion of chars is expected to be lower for oxy-fuel combustion than for air-combustion.

2. Experiments

The aim of this paper is to present experimental results of NO_X formation in oxy-fuel combustion of lignite in a 30 kW_{th} BFBC with real flue gas recirculation (FGR) simulating conditions in real combustors and their comparison with a simplified 1-D mathematical model of oxy-fuel combustion in a bubbling fluidized bed using a plug-flow reactor (PFR) model. This model is used to discuss the achieved experimental results. Within the experiments, the Czech lignite coal 'Bílina' was used as fuel. The composition of this lignite is given in Table 1, which is also the composition that was used in the numerical simulations. The particle size distribution of the coal was in the range from 0 to 8 mm. The experiments were carried out in a 30 kW_{th} lab-scale BFB combustor, which has already been described elsewhere (Hrdlicka et al., 2016). Its scheme is given in Fig. 1. It has a modular construction made of stainless steel. The height of the combustor is 2.7 m (2.2 m from the fluidizing gas distributor to the top of the reactor) and its cross-section is 0.15 × 0.225 m in the fluidized bed section and 0.3 × 0.2 m in the freeboard section. The facility can operate in both air- and oxy-combustion mode. In the oxy-fuel combustion regime, pure oxygen from pressurized or cryogenic vessels is used as an oxidizer and the bed material (fuel ash – 0.37 mm) is fluidized by the mixture of recirculated flue gas and oxygen. The FGR is taken from downstream flue gas, after cyclone separator, through two water coolers to the suction pipe of the primary fan. At the output from the primary fan, the oxygen is mixed with the recirculated flue gas. The composition of the flue gas is continuously analysed by an on-line gas analyser. The measured sample is taken from the flue gas vent pipe between the cyclone separator and the flue gas fan. The volumetric fractions of CO_2, O_2, CO, SO_2 and NO_X ($NO + NO_2$) are measured. The vertical profile of temperature along the combustor is measured using five thermocouples in the fluidized bed section and three thermocouples in the freeboard section.

3. Modelling

A simple 1-D mathematical model of the BFBC was proposed using a plug flow reactor concept to bring deeper understanding of the experimental results. To provide comparable outputs, the dimensions and operating parameters of the PFR were set according to the corresponding parameters of the experimental facility. The scheme of the PFR is given in Fig. 2. The superficial gas velocity, the fuel load, as well as the temperature, were set as the source terms according to the measured data. The previous experiments shown that the temperature in the fluidized bed does not change much with the height (up to 10 °C), so the in-bed temperature was also considered independent on height. Above the bed, the temperature decreases because the heat loss to the reactor walls is higher than the heat released from the oxidation of the remaining combustibles. The absolute value of the temperature decrease between fluidized bed and outlet from the combustor varies in time of operation (from 250 to 320 °C) and depends mostly on the runtime of the facility, particularly due to the accumulation abilities of the insulation and the stainless steel construction and subsequent increased heat convection, because the combustor is not operated continuously in term of days. The value of 260 °C was used in the model as the typical temperature drop between the bed and combustor outlet. Moreover, calculation of the heat losses showed that such value could be expected in steady state combustion.

The numerical model is based on calculation of homogeneous combustion reaction kinetics using the GRI-mech 3.0 mechanism (Smith et al., 2018). This mechanism was designed to model natural gas combustion, including NO formation and re-burning, and contains 325 reactions and 53 species. The simplification introduced by neglecting the heterogeneous char reactions was compensated by including typical char combustion products in the volatiles. The grid of the numerical PFR reactor model was based on time steps. The duration of each time step was chosen according the residence time of the gas – differently in the fluidized bed zone (0.00016 s) and in the freeboard zone (0.0054 s) providing 800 steps in the fluidized bed and 200 steps in the freeboard section. The devolatilisation takes place in each step of the fluidized bed zone in an amount equivalent to the fuel load at the time step. The composition of volatiles after devolatilisation and char combustion was determined using data published by Winter et al. (1996) and Konttinen et al. (2013), fuel properties and the stoichiometry of the oxy-fuel combustion. The corresponding compositions that are used in the numerical simulations are given in Table 2. The distribution of coal elements between chars and volatiles was estimated based on the ultimate analysis of the 'Bílina' lignite and devolatilisation coefficients calculated from the data for brown coal published by Konttinen et al. (2013) Then, the distribution of nitrogen compounds between chars and volatiles was calculated using the nitrogen compounds conversion rates for sub-bituminous coal published by (Winter et al., 1996). The formation of volatile carbon compounds from the volatile carbon was considered with shares 0.35, 0.25, 0.35 and 0.05 for CH_4, C_2H_6, CO and CO_2. The production of O_2 and H_2 was calculated from the remaining shares of H and O in the chars and volatiles. The GRI-mech does not include sulphur and its reactions, however this disadvantage can be accepted, since the sulphur does not affect the nitrogen chemistry significantly. The numerical model computes only the gas composition, flow rate and velocity and does not respect the fluidized bed hydrodynamics and gas-solid heat transfer. The gas velocity in the PFR reflects the voidage in the fluidized bed, devolatilisation of fuel and the changes of temperature. As already mentioned, the model is simplified and is not intended to provide detailed modelling of the fluidized bed oxy-fuel combustion process. However, the results show, that despite this it can be possibly used to explain the tendencies observed within the experiments.

The flue gas recirculation (FGR) is respected in the calculation through a number of iterations, where the output composition of flue gas is used as the source term for computation of FGR composition, where the content of water vapour depends on the FGR temperature measured within the experiments.

4. Results

4.1. Experimental results

To observe the trends in NO_X formation, several measurements have been made while varying only one single parameter. While studying the influence of fluidized bed temperature, the oxygen excess was kept constant at a volume fraction in the dry flue gas of 6%. The fluidized bed temperature was controlled through the change of the FGR flow or the change of the fuel load in cases where the FGR was inefficient. These process control changes can cause differences in O_2 concentration at the inlet gas or differences in the gas residence times along the series of experiments and so some unwanted side-effects. However, it is very important to notice that these were the only possible means to control

Table 1
Proximate and ultimate analysis of Czech lignite 'Bílina' (standards used for the fuel analysis: LHV – ČSN ISO 1928, water content – ČSN 44 1377, ash content – ČSN ISO 1171; ultimate analysis determined by Thermo Scientific FlashEA 112).

As received			Dry ash free			
LHV [MJ/kg]	Water [wt. %]	Ash [wt. %]	C [wt. %]	H [wt. %]	N [wt. %]	S [wt. %]
17.6	21.1	9.9	72.3	6.3	1.1	1.3

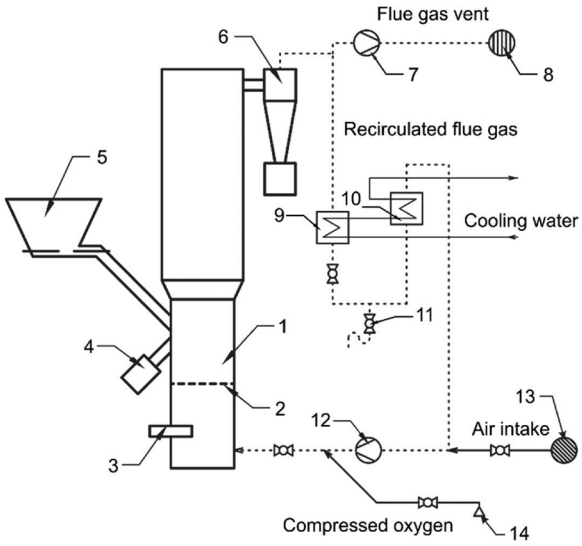

Fig. 1. Scheme of the 30 kW_{th} BFB experimental facility. 1) fluidized bed region, 2) distributor of the fluidizing gas, 3) gas burner mount, 4) fluidized bed spillway, 5) fuel feeder, 6) cyclone separator, 7) flue gas fan, 8) flue gas vent, 9) and 10) water coolers, 11) condensate drain, 12) primary fan, 13) air-suck pipe, 14) vessels with oxygen.

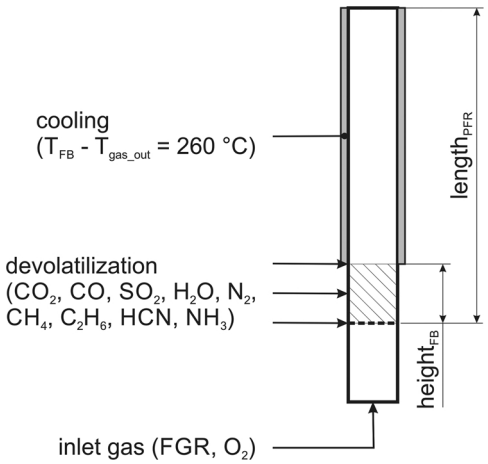

Fig. 2. Scheme of the plug flow reactor model.

Table 2
Distribution of lignite species between chars and volatiles and the production of compounds from devolatilisation and char combustion of 1 kg of fuel.

		char	volatiles
C	dry ash-free	44.35	28.87
H		0.39	6.04
N	[% wt.]	0.69	0.46
O		2.88	16.33
NH_3	[g/kg_{fuel}]	0.14	0.93
HCN		0.16	0.31
NO		0.84	1.24
N_2O		0.02	0.09
N_2		4.08	1.54
CH_4		–	68.76
C_2H_6		–	49.11
CO		30.18	68.76
H_2		2.59	13.56
O_2		18.99	71.05
CO_2		1059.41	278.97
H_2O			211.20

the fluidized bed temperature and these are the only possible means of controlling real scale combustors. Four steady cases with bed temperatures of 840, 880, 920 and 960 °C have been measured for 40 min each time. The mean values of the relevant parameters are found in Table 3, referenced as 'case 1', 'case 2', 'case 3' and 'case 4' respectively. On the other hand, the influence of the oxygen excess was measured while keeping the fluidized bed temperature constant (at approximately 880 °C) and changing the flow of the oxygen entering the system. The temperature was regulated through the change of the FGR flow when necessary. The mean values of steady cases are given in Table 3, referenced as 'case 5', 'case 2' and 'case 6' for the volumetric fractions of the oxygen in the dry flue gas equal approx. to 3, 6 and 9% respectively.

Within the experiments, the NO_X formation is found to be sensitive towards the excess of oxygen, as can be seen in Fig. 3. With increase of the oxygen volumetric fraction in the dry flue gas from 3% to 9%, the NO_X emission raises from 336 to 469 ppm (increment of approximately 40%). On the other hand, for a constant oxygen concentration, no significant impact of the fluidized bed temperature was observed within the results presented in the Table 3. The NO_X volumetric fraction in the dry flue gas varies between 394 and 419 ppm within the temperature range 840–960 °C, but with no obvious correlation. However, as can be seen, the volumetric fraction of CO was considerably raised in cases 3 and 4, although the concentration of oxygen in the dry flue gas was almost at the same level as in cases 1 and 2. The higher CO concentration could enhance the NO_X reduction and diminish the temperature sensitivity of the NO_X formation. Therefore, additional experiments, examining the impact of fluidized bed temperature on the NO_X formation, were performed. This time, five steady states were measured twice for temperatures 800, 840, 880, 920 and 960 °C for basically the same conditions as in cases 1–4. All experimental results are compared in the Fig. 4, where the original data are represented by black filled circles. Detail results of the two supplementary measured temperature profiles can be found in the appendix referred as cases 7–16.

4.2. Numerical results

To study the NOx formation tendencies and concentration profiles along the reactor height, the results from the mathematical model were evaluated for the same conditions as used in the experiments, e.g. four temperatures and three O_2 volumetric fractions in dry flue gas, even if the numerical solution enables us to show the continuous relations. To compare numerical and experimental results, values found at the top of the reactor (2 m) have to be used since the probe of the gas analyser was placed there within the experiments.

The results obtained from the numerical simulations are reported as overall NO_X emission, although the numerical model can calculate the formation of NO and NO_2 separately. This is because the experimental measurement using NDIR gas analyser provides information only about the overall NO_X concentration, since the NO_2 molecules are reduced to NO in a catalyser and thus the NO_2 concentration cannot be directly measured continuously together with NO and the numerical results cannot be verified experimentally. The progress of NO_X formation in correlation with the excess of oxygen is described in Fig. 5. Here, each line represents different O_2 volumetric fraction in dry flue gas. The impact of the fluidized bed temperature on the NO_X formation can be seen in Fig. 6. Here, the same temperature range as in the original experiments was used. In addition, one significantly higher temperature (1360 °C) was also included to show the hypothetical further development. However, this situation cannot happen in real practice. At such temperature, the ash present in the BFB would melt and the BFB material would agglomerate. The x-axes of the charts in Figs. 5 and 6 are in log-scale to highlight changes in fluidized bed, since the correlations in the freeboard are more clear. However, the values in the leftmost part of the charts (from 0 to 0.001 m) are not relevant, because the numerical model does not provide reasonable data at such small distances

Table 3
Experimental data: NO_X formation in dependence on fluidized bed temperature and on the oxygen excess. The volumetric fractions of the flue gas components listed in the table are measured from dry flue gas.

		case 1	case 2	case 3	case 4	case 5	case 6
t_{FB}	[°C]	842	886	923	962	886	882
t_{OUT}	[°C]	582	615	650	651	563	627
t_{FGR}	[°C]	68	72	74	74	94	76
ω_{CO2}	[vol. %]	88.9	89.9	89.2	89.3	92.5	87.0
ω_{O2}	[vol. %]	6.8	6.1	6.1	6.1	2.9	8.5
ω_{NOx}	[ppmv]	394	419	414	419	336	469
ω_{CO}	[ppmv]	522	612	1121	1021	3042	516
ω_{CO}/ω_{CO2}	[-]	0.57×10^{-3}	0.68×10^{-3}	1.26×10^{-3}	1.14×10^{-3}	3.29×10^{-3}	0.59×10^{-3}
res. t_{FB}	[s]	0.29	0.27	0.25	0.26	0.27	0.27
res. $t_{freeb.}$	[s]	3.64	3.34	3.12	3.33	3.32	3.52
res. $t_{overall}$	[s]	3.93	3.61	3.38	3.59	3.59	3.79
O_2/CO_{2_IN}	[-]	0.16	0.16	0.16	0.18	0.19	0.26
u_0/u_{mf}	[-]	3.38	3.76	4.10	4.01	3.75	3.74

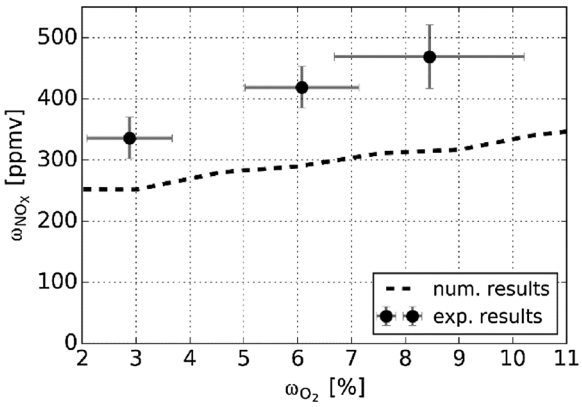

Fig. 3. Experimental data (including standard deviations) and numerical results: Dependence of NO_X formation on the oxygen excess. The fluidized bed temperature was in all cases about 880 °C.

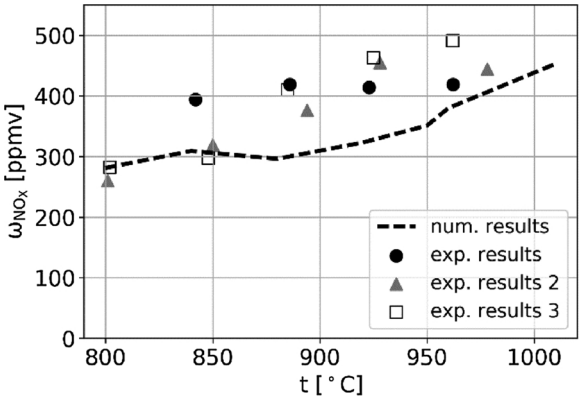

Fig. 4. Experimental data and numerical results: Dependence of NO_X formation on FB temperature. The volumetric fraction of O_2 in dry flue gas was in all cases about 6%. The supplementary measured data are referred as the experimental results 2 and 3.

(de las Obras-Loscertales et al., 2015).

5. Discussion

5.1. Effect of the oxygen excess

The NO_X is formed mainly through the oxidation of fuel-bound nitrogen, hence the oxygen excess is obviously of importance when examining the key parameters affecting the NO_X formation. In addition to the fact that the O_2 concentration affects the kinetics of the oxidation

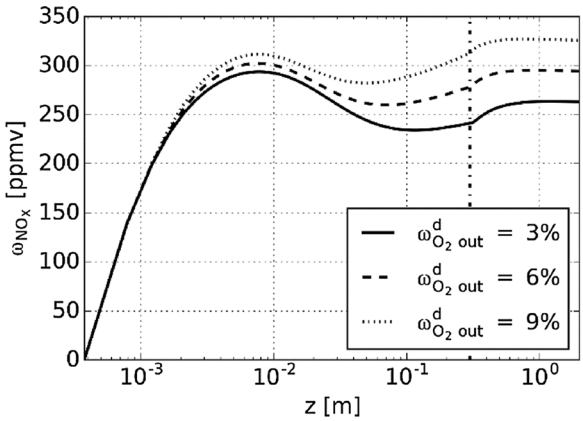

Fig. 5. Numerical model: Development of NO_X concentration along the height of the reactor in dependence on oxygen excess. The leftmost point indicates the bottom of the reactor – the distributor of the fluidizing gas. The vertical dash-and-dot line indicates the surface of the fluidized bed. The height of the reactor "z" is in log-scale.

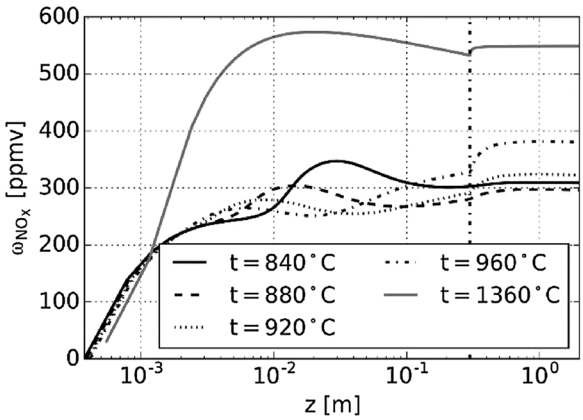

Fig. 6. Numerical model: Development of NO_X concentration along the height of the reactor in dependence on fluidized bed temperature. The vertical dash-and-dot line indicates the surface of the fluidized bed. The leftmost point indicates the bottom of the reactor – the distributor of the fluidizing gas. The height of the reactor "z" is in log-scale.

reactions of NO_X precursors, it also affects the peak temperature of the char particles and the CO concentration in the flue gas. While the peak temperature of the char raises with increasing O_2 concentration, which promotes the char-N to NO_X conversion, the CO concentration in the flue gas decreases, which inhibits the already formed NO_X reduction. The numerical results of the overall volumetric fraction of NO_X, as a

function of height in the reactor, is given in Fig. 5. Here, the obvious impact of the excess of oxygen can be seen. The NO_X fraction at the reactor outlet increases from 263 ppm to 323 ppm as the O_2 fraction is increased from 3 to 9%, which is an increment of approx. 23%. That is not as much as observed in the experiments (increment of 40% from 336 to 469 ppm), but the trends are the same as can be seen in Fig. 3. Although the numerical results do not match the experimental results exactly, they are still in very good agreement. The observed differences can be explained by the low dimensionality of the numerical approach and by the possibly inaccurate composition of volatiles, which was determined using data published for a different type of lignite. Therefore, the model should be used rather to compare trends than the absolute values.

5.2. Effect of BFB temperature

The impact of fluidized bed temperature on the overall NO_X production in the temperature range used in the original experiments seemed to be indefinite, although at higher temperatures the numerical model is strongly temperature-dependent, as can be seen in Fig. 6. Since the CO concentration was significantly raised for temperatures of 920 and 960 °C within the experiments, supplementary measurements were done where the CO concentration was kept low (from 60 to 290 ppmv). For these measurements the NO_X formation showed significant fluidized bed temperature dependence. The NO_X fraction at the reactor outlet increased from 282 ppm to 491 ppm (increment of 74%) as the fluidized bed temperature increased from 802 to 962 °C. The comparison of the experimental and numerical data can be seen in the Fig. 4. The temperature range used in the numerical model was extended to cover temperatures from 800 to 1010 °C. Although the results seem to be in good agreement, the impact of the fluidized bed temperature on the NO_X formation can be easily diminished by the increase of the CO concentration due to the enhanced Boudouard reaction, as was observed within the original experimental data. Therefore, the temperature dependence of the NO_X formation in oxy-fuel combustion in fluidized beds is currently being actively discussed in the open literature. For example Lupiáñez et al. (2013) and de las Obras-Loscertales et al. (2015), who did experiments on lab-scale BFB combustors with FGR made from a mixture of clean gases, did not observe any temperature sensitivity.

6. Conclusions

The impact of oxygen excess and fluidized bed temperature on NO_X formation in oxy-fuel combustion of lignite was studied using a numerical PFR model and the results were validated against experiments performed in a 30 kW_{th} BFBC. Both the numerical and the experimental results show significant sensitivity on the excess of oxygen, where higher O_2 concentrations enhance the oxidation of the fuel-bound nitrogen, resulting in an increase of the overall NO_X concentration in the flue gas. In addition, a significant fluidized bed temperature dependence of the NO_X formation was observed both in the numerical and the experimental results.

Acknowledgments

This work was supported by Norway Grants 2009–2014, under CZ08 Programme, Fund for Bilateral Relations at Programme Level, Initiative No. NF-CZ08-BFB-1-026-2017 and by the Grant Agency of the Czech Technical University in Prague, grant No. SGS16/211/OHK2/3T/12 which are gratefully acknowledged.

Appendix A

See Table A1.

Table A1
Supplementary experimental data: NO_X formation in dependence on the fluidized bed temperature.

		experimental results 2				
		case 7	case 8	case 9	case 10	case 11
t_{FB}	[°C]	801	850	894	928	978
t_{FB_dev}	[°C]	11	5	3	9	4
t_{OUT}	[°C]	690	697	729	723	733
t_{FG_rec}	[°C]	82	81	84	77	64
ω_{CO2}	[vol. %]	86.7	86.2	87.2	86.6	87.3
ω_{O2}	[vol. %]	6.1	6.3	6.3	7.0	6.6
ω_{O2_dev}	[vol. %]	1.9	1.2	1.1	2.0	1.0
ω_{NOx}	[ppmv]	260	319	376	455	444
ω_{NOx_dev}	[ppmv]	57	37	38	73	37
ω_{CO}	[ppmv]	186	186	146	61	158
ω_{CO_dev}	[ppmv]	185	27	104	53	131
ω_{CO}/ω_{CO2}	[-]	0.1×10^{-3}	0.22×10^{-3}	0.17×10^{-3}	0.7×10^{-4}	0.18×10^{-3}
		experimental results 3				
		case 12	case 13	case 14	case 15	case 16
t_{FB}	[°C]	802	848	885	925	962
t_{FB_dev}	[°C]	15	4	9	7	3
t_{OUT}	[°C]	651	703	701	726	738
t_{FG_rec}	[°C]	93	78	78	83	79
ω_{CO2}	[vol. %]	87.4	89.0	87.4	87.7	87.8
ω_{O2}	[vol. %]	6.0	5.0	6.5	6.5	6.4
ω_{O2_dev}	[vol. %]	1.4	1.1	1.8	1.5	1.3
ω_{NOx}	[ppmv]	282	297	410	463	491
ω_{NOx_dev}	[ppmv]	40	38	74	67	56
ω_{CO}	[ppmv]	289	242	84	168	165
ω_{CO_dev}	[ppmv]	117	460	111	244	130
ω_{CO}/ω_{CO2}	[-]	0.33×10^{-3}	0.27×10^{-3}	0.96×10^{-4}	0.19×10^{-3}	0.19×10^{-3}

References

Bhunia, S., Sadhukhan, A.K., Gupta, P., 2017. Modelling and experimental studies on oxy-fuel combustion of coarse size coal char. Fuel Process. Technol. 158.

de las Obras-Loscertales, M., et al., 2015. NO and N2O emissions in oxy-fuel combustion of coal in a bubbling fluidized bed combustor. Fuel 150, 146–153.

Duan, L., Zhao, C., Ren, Q., Wu, Z., Chen, X., 2011. NOx precursors evolution during coal heating process in CO 2 atmosphere. Fuel 90 (4), 1668–1673.

Giménez-López, J., Millera, A., Bilbao, R., Alzueta, M.U., 2010. HCN oxidation in an O_2/CO_2 atmosphere: an experimental and kinetic modeling study. Combust. Flame 157 (2), 267–276.

Glarborg, P., Jensen, A.D., Johnsson, J.E., 2003. Fuel nitrogen conversion in solid fuel fired systems. Prog. Energy Combust. Sci. 29 (2), 89–113.

Hrdlicka, J., Skopec, P., Opatril, J., Dlouhy, T., 2016. Oxyfuel combustion in a bubbling fluidized bed combustor. Energy Procedia 86, 116–123.

Jensen, A., Johnsson, J.E., Dam-Johansen, K., 1996. Nitrogen chemistry in FBC with limestone addition. Twenty-Sixth Symp. Combust. Combust. Inst. 1, 3335–3342.

Johnsson, J.E., 1994. Formation and reduction of nitrogen oxides in fluidized-bed combustion. Fuel 73 (9), 1398–1415.

Konttinen, J., Kallio, S., Hupa, M., Winter, F., 2013. NO formation tendency characterization for solid fuels in fluidized beds. Fuel 108, 238–246.

Li, C.Z., Nelson, P.F., 1996. Interactions of quartz, zircon sand and stainless steel with ammonia: implications for the measurement of ammonia at high temperatures. Fuel 75 (4), 525–526.

Li, C.Z., Nelson, P.F., Ledesma, E.B., Mackie, J.C., 1996. An experimental study of the release of nitrogen from coals pyrolyzed in fluidized-bed reactors. Symp. Combust. 26 (2), 3205–3211.

Lupiáñez, C., Guedea, I., Bolea, I., Díez, L.I., Romeo, L.M., 2013. Experimental study of SO_2 and NOx emissions in fluidized bed oxy-fuel combustion. Fuel Process. Technol. 106 (x), 587–594.

Mahmoudi, S., Baeyens, J., Seville, J.P.K., 2010. NOx formation and selective non-catalytic reduction (SNCR) in a fluidized bed combustor of biomass. Biomass Bioenergy 34 (9), 1393–1409.

Normann, F., Andersson, K., Leckner, B., Johnsson, F., 2009. Emission control of nitrogen oxides in the oxy-fuel process. Prog. Energy Combust. Sci. 35 (5), 385–397.

Salinero, J., Gómez-Barea, A., Fuentes-Cano, D., Leckner, B., 2018. The influence of CO2 gas concentration on the char temperature and conversion during oxy-fuel combustion in a fluidized bed. Appl. Energy 215 (April), 116–130.

Skopec, P., Hrdlička, J., Opatřil, J., Štefanica, J., 2015. NOx emissions from bubbling fluidized bed combustion of lignite coal. Acta Polytech. 55 (4), 275.

Smith, G.P., et al., 2017. GRI- MECH 3.0. [Online]. Available:. [Accessed: 08-Aug-2017]. http://www.me.berkeley.edu/gri_mech/.

Svoboda, K., Hartman, M., Pohořelý, M., Trnka, O., 2004. modelling of effects of operating conditions and coal reactivity on temperature of burning particles in fluidized bed combustion. Acta Geodyn. Geomater. 1 (2), 261–274.

Toftegaard, M.B., Brix, J., Jensen, P.A., Glarborg, P., Jensen, A.D., 2010. Oxy-fuel combustion of solid fuels. Prog. Energy Combust. Sci. 36 (5), 581–625.

United Nations and Canada, 1992. United Nations Framework Convention on Climate Change. United Nations, General Assembly, New York.

Winter, F., Wartha, C., Löffler, G., Hofbauer, H., 1996. The NO and N2O formation mechanism during devolatilization and char combustion under fluidized-bed conditions. Symp. Combust. 26 (2), 3325–3334.

Zhou, H., Li, Y., Li, N., Qiu, R., Cen, K., 2018. Conversions of fuel-N to NO and N2O during devolatilization and char combustion stages of a single coal particle under oxy-fuel fluidized bed conditions. J. Energy Inst.(Jan).

Zhu, C., Liu, S., Liu, H., Yang, J., Liu, X., Xu, G., 2015. NOx emission characteristics of fluidized bed combustion in atmospheres rich in oxygen and water vapor for high-nitrogen fuel. Fuel 139, 346–355.